I. BEHAVIOR OF A GENERALIZED SYSTEM WITH A NEGATIVE FEEDBACK

Consider a simple linear ordinary differential equations (ODE) system:

$$\begin{aligned} \dot{x} &= S - \alpha x - \beta y, \\ \dot{y} &= \gamma x - \delta y, \end{aligned} \qquad [1]$$

This represents a simple differential equations approximation of a biochemical system with a negative feedback. It captures, however, main aspects of more complex equations systems with a single negative feedback interaction. In this system the molecular species *x* and *y* interact in such a way that *x* is negatively regulated by *y*, whereas y is positively regulated by *x*. In addition, self-regulation of x and y is included and considered to be negative. Biochemically speaking, x activates *y*, whereas *y* feeds negatively back to *x*. In addition, *x* and y are constitutively downregulated, e.g., by degradation. The Greek letters represent non-negative rate constants. The external signal *S* determines the degree of activation of the entire system.

Treatment of linear ODE systems can be found in most standard differential equations textbooks (for a good example of comprehensive ODE–Based treatment of biological data see L. Edelstein-Koshet, Mathematical Models in Biology, McGraw Hill, New York, NY, 1988). The behavior of [1] is determined by the values of parameters: $a = -\alpha - \delta$ and $b = \alpha\delta+\beta\gamma$. We note that we always have: $a \leq 0$ and $b \geq 0$. These conditions lead to two possible "phase portraits" of the system: the stable spiral or the stable node. The stable spiral implies damped oscillations for the values of both x and y when plotted as a function of time as both variables approach the stable steady state determined by S. The stable spiral is actualized if $a^2 < 4b$. In other words, the lower the value of a compared to *b*, the more "oscillatory" or less damped the behavior. The limiting case of $a = 0$ (corresponding to "center", see above) generates undamped oscillations. A related result is that the value of *a* determines how fast the system relaxes to the steady state value, whereas the value of *b* determines the frequency of the oscillations.

The above treatment interpreted biochemically means that the higher the feedback regulation terms (represented by *b*) compared to self-regulation terms (represented by *a*), the less damped (or more pronounced) is the oscillatory response to changes in the external signal *S.* The frequency of the oscillations is inversely proportional to *b*. Therefore an increase in system parameters determining *b* for [1] will strengthen the negative feedback but will also increase the propensity for oscillations in the response. In some biochemical systems with negative feedbacks oscillations can thus arise as a by-product of the necessity of fast signal down-regulation.

II. DESCRIPTION OF THE MODEL

Introduction

The focus of the model is the central signaling module that appears to transduce all NF-κB responses. It consists of IKK represented here as a single signaling entity (without separate descriptions for IKK1/IKK2 (IKKα/IKKβ) heterodimer scaffolded by NEMO (IKKγ)), three mammalian IκB isoforms (α,β and ε), and NF-κB. NF-κB heterodimer isoforms are not specified in this model, a simplification that has two justifications: (1) A single NF-κB isoform (p50/p65) with transcriptional activation potential predominates in many cells. (2) IκB-NF-κB interaction appears to be promiscuous with little molecular preferences evident in NF-κB/Rel or IκB protein knockouts (A. Hoffmann, unpublished data). While future version of the model may consider the substructure of multi-protein complexes, the present model is adequate in addressing the role of different IκB isoforms in controlling the dynamic response of the pathway to transient and persistent stimulation.

The model consists of a series of ordinary differential equations describing the time evolution of concentrations of various molecules and molecular complexes of interest. In particular, nuclear NF-κB, bimolecular IKK-IκB, IκB-NF-κB and trimolecular IKK-IκB-NF-κB complexes for each IκB isoform are explicitly considered. The participating molecular species are assumed to translocate between two subcellular compartments: the cytoplasm and the nucleus, thus necessitating considerations about transport rates in addition to binding and reaction rates. The input into the signaling module is represented by the concentration of the active IKK. This assumption allows the model to be applied to a variety of ligands – different ligands may, however, lead to different IKK activation profiles via signaling modules that are not subject of this study. Further, we assumed that ubiquitination and proteolysis of IκB isoforms follows immediately the specific phosphorylation event of IκB by IKK. While we can represent the whole process by a single reaction rate here, future versions of the model will distinguish between these steps as more biochemical data becomes available. Thus the interaction of IKK and IκB isoforms effectively proceeds as a single enzymatic degradation reaction scheme:

$$E + S \rightleftharpoons ES \rightarrow E,$$

where E is the enzyme, S is the substrate and ES is the enzyme-substrate complex. This reaction scheme gives rise to three differential equations describing the rates of change of the concentrations of E, S and ES.

In the computational model all four rates are described explicitly. In general, enzymes, substrates and products of individual reactions can be shared among multiple reactions giving rise to more complex differential equations for the corresponding concentrations. Thus, in order to describe changes in the concentration of a reaction component completely, all reactions that this component participates in, plus possible transport, degradation and complex formation rates must be considered.

Nomenclature

Uppercase letters denote concentrations of molecular species. All are proteins, except those subscripted with t, which are relevant messenger RNA transcripts.
Lower case letters with numbers represent the corresponding model parameters.
Uncomplexed molecules are described by the designated symbol immediately followed by (t).
Complexes of molecules are described by the designated symbols of their component molecules written next to each other without separation by (t).
The subscripted *n* indicates that the molecule is in the nucleus.

Free cytoplasmic NF-κB protein

The first two lines represent the depletion of free NF-κB due to formation of IκB-NF-κB complexes (the terms containing the association rate constants a4, a5, a6) and formation of free NF-κB due to dissociation of these complexes (the terms containing the dissociation rate constants d4, d5, d6).
The next three lines describe the changes in the concentration of free NF-κB due to binding to and dissociation from binary IKK-IκB complexes and freeing of NF-κB due to IκB degradation in these complexes following its phosphorylation by IKK (the reaction rate terms are r4, r5 and r6).
The next line describes the rate of degradation of IκB isoforms in IκB-NF-κB complexes (the terms with the degradation rate constant deg4 assumed to be equal for all the isoforms).
The final line of the equation represents the first order transport terms for the transport of NF-κB into (the rate constant k1) and out of the nucleus (the rate constant k01).

$$
\begin{aligned}
&\textit{NF-}\kappa B'(t) = \ -a4\ I\kappa B\alpha(t)\ \ \textit{NF-}\kappa B(t) + d4\ I\kappa B\alpha\ \textit{NF-}\kappa B(t) - a5\ I\kappa B\beta(t)\ \ \textit{NF-}\kappa B(t) + d5\ I\kappa B\beta\ \textit{NF-}\kappa B(t)\\
&-a6\ I\kappa B\varepsilon(t)\ \ \textit{NF-}\kappa B(t) + d6\ I\kappa B\varepsilon\ \textit{NF-}\kappa B(t)\\
&-a4\ \textit{IKK}I\kappa B\alpha(t)\ \ \textit{NF-}\kappa B(t) + (r4 + d4)\ \textit{IKK}I\kappa B\alpha\ \textit{NF-}\kappa B(t)\\
&-a5\ \textit{IKK}I\kappa B\beta(t)\ \ \textit{NF-}\kappa B(t) + (r5 + d5)\ \textit{IKK}I\kappa B\beta\ \textit{NF-}\kappa B(t)\\
&-a6\ \textit{IKK}I\kappa B\varepsilon(t)\ \ \textit{NF-}\kappa B(t) + (r6 + d6)\ \textit{IKK}I\kappa B\varepsilon\ \textit{NF-}\kappa B(t)\\
&+deg4\ I\kappa B\alpha\ \textit{NF-}\kappa B(t) + deg4\ I\kappa B\beta\ \textit{NF-}\kappa B(t) + deg4\ I\kappa B\varepsilon\ \textit{NF-}\kappa B(t)\\
&-k1\ \ \textit{NF-}\kappa B(t) + k01\ \ \textit{NF}-\kappa B_n(t),
\end{aligned}
$$

Free nuclear NF-κB protein

The terms describe transport into and out of the nucleus, and sequestration through nuclear IκB isoforms.

$$
\begin{aligned}
&\textit{NF}-\kappa B_n'(t) = \ k1\ \textit{NF}-\kappa B(t) - a4\ I\kappa B\alpha_n(t)\ \ \textit{NF}-\kappa B_n(t) + d4\ I\kappa B\alpha_n\ \textit{NF}-\kappa B_n(t) -\\
&\quad a5\ I\kappa B\beta n(t)\ \ \textit{NF}-\kappa B_n(t) + d5\ I\kappa B\beta_n\ \textit{NF}-\kappa B_n(t) - a6\ I\kappa B\varepsilon_n(t)\ \ \textit{NF}-\kappa B_n(t) +\\
&\quad d6\ I\kappa B\varepsilon_n\ \textit{NF}-\kappa B_n(t) - k01\ \ \textit{NF}-\kappa B_n(t),
\end{aligned}
$$

IκB mRNA transcript levels

An accurate mathematical account of regulation of transcription and translation is difficult because of inherent complexity of the underlying regulatory processes that are still to a large measure unknown. We have thus given simple semi-qualitative descriptions of the dependence of the rates of transcription and translation on the concentration of NF-κB and the concentration of IκB transcripts. We have opted to include separate descriptions of transcription and translation since the data on mRNA concentration as a function of time are increasingly available through DNA microarray and other technologies. The transcription of IκB isoforms was assumed to be a second order process proportional to the square of nuclear NF-κB concentration for IκBα and zero order constitutive processes for all three isoforms. The second order dependence of inducible IκBα transcription was introduced to capture the fact that NF-κB is a dimer and as such can be presumed to bind DNA in a non-linear, cooperative fashion. This non-linearity, however, is not essential for the qualitative behavior of the model, as can be easily shown computationally. The degradation of IκB mRNA transcripts was described according to unsaturable first order kinetics for all isoforms. The sensitivity of the model to variations of the synthesis and degradation rates is examined in Supplement 3 and Fig. 6 of the paper.

$$I\kappa B\alpha_t'(t) = tr2a + tr2\ \ \textit{NF}-\kappa Bn(t)^2 - tr3\ I\kappa B\alpha_t(t),$$

$$I\kappa B\beta_t'(t) = tr2b - tr3\ I\kappa B\beta_t(t),$$

$$I\kappa B\varepsilon_t'(t) = tr2e - tr3\ I\kappa B\varepsilon_t(t),$$

Free cytoplasmic IκB proteins

The equations account for cytoplasmic sequestration by IKK (association and dissociation rate constants: a1 and d1 for IκBα, a2 and d2 for IκBβ and a3 and d3 for IκBε) and NF-κB, nuclear transport (with the rate of import tp1 and export tp2 assumed to be equal for all isoforms), synthesis (the rate of translation tr1) and constitutive degradation (deg1 assumed to be equal for all isoforms).

$$IκBα'(t) = -a1\ IKK(t)\ IκBα(t) + d1\ IKKIκBα(t) - a4\ IκBα(t)\ \ NF{-}κB(t) + d4\ IκBα\ NF{-}κB(t) + tr1\ IκBα_t(t) - deg1\ IκBα(t) - tp1\ IκBα(t) + tp2\ IκBα_n(t),$$

$$IκBβ'(t) = -a2\ IKK(t)\ IκBβ(t) + d2\ IKKIκBβ(t) - a5\ IκBβ(t)\ \ NF{-}κB(t) + d5\ IκBβ\ NF{-}κB(t) + tr1\ IκBβ_t(t) - deg1\ IκBβ(t) - 0.5\ tp1\ IκBβ(t) + 0.5\ tp2\ IκBβ_n(t),$$

$$IκBε'(t) = -a3\ IKK(t)\ IκBε(t) + d3\ IKKIκBε(t) - a6\ IκBε(t)\ \ NF{-}κB(t) + d6\ IκBε\ NF{-}κB(t) + tr1\ IκBε_t(t) - deg1\ IκBε(t) - 0.5\ tp1\ IκBε(t) + 0.5\ tp2\ IκBε_n(t),$$

Free nuclear IκB proteins

Nuclear concentrations of IκB isoforms are determined by nuclear transport and binding to nuclear NF-κB.

$$IκBα_n'(t) = tp1\ IκBα(t) - tp2\ IκBα_n(t) - a4\ IκBα_n(t)\ \ NF{-}κB_n(t) + d4\ IκBα_n\ NF{-}κB_n(t),$$

$$IκBβ_n'(t) = 0.5\ tp1\ IκBβ(t) - 0.5\ tp2\ IκBβ_n(t) - a5\ IκBβ_n(t)\ \ NF{-}κB_n(t) + d5\ IκBβ_n\ NF{-}κB_n(t),$$

$$IκBε_n'(t) = 0.5\ tp1\ IκBε(t) - 0.5\ tp2\ IκBε_n'(t) - a6\ IκBε_n(t)\ \ NF{-}κBn(t) + d6\ IκBε_n\ NF{-}κBn(t),$$

Cytoplasmic IκB-NF-κB complexes

Their presence is determined by binding rates and constitutive IκB degradation.

$$IκBα\ NF{-}κB'(t) = a4\ IκBα(t)\ \ NF{-}κB(t) - d4\ IκBα\ NF{-}κB(t) - a7\ IKK(t)\ IκBα\ NF{-}κB(t) + d1\ IKKIκBα\ NF{-}κB(t) + k2\ IκBα_n\ NF{-}κB_n(t) - deg4\ IκBα\ NF{-}κB(t),$$

$$IκBβ\ NF{-}κB'(t) = a5\ IκBβ(t)\ \ NF{-}κB(t) - d5\ IκBβ\ NF{-}κB(t) - a8\ IKK(t)\ IκBβ\ NF{-}κB(t) + d2\ IKKIκBβ\ NF{-}κB(t) + 0.4\ k2\ IκBβ_n\ NF{-}κB_n(t) - deg4\ IκBβ\ NF{-}κB(t),$$

$$IκBε\ NF{-}κB'(t) = a6\ IκBε(t)\ \ NF{-}κB(t) - d6\ IκBε\ NF{-}κB(t) - a9\ IKK(t)\ IκBε\ NF{-}κB(t) + d3\ IKKIκBε\ NF{-}κB(t) + 0.4\ k2\ IκBε_n\ NF{-}κB_n(t) - deg4\ IκBε\ NF{-}κB(t),$$

Nuclear IκB-NF-κB complexes

The equations above are balanced by the corresponding equations describing the formation of the nuclear IκB-NF-κB complexes. IκBβ-NF-κB and IκBε-NF-κB complexes are transported with the rates equal to 0.5 of the rate of IκBα-NF- κB complexes (tp2). (see Parameter Estimation)

$$IκBα_n\ NF{-}κB_n'(t) = a4\ IκBα_n(t)\ \ NF{-}κBn(t) - d4\ IκBα_n\ NF{-}κB_n(t) - k2\ IκBα_n\ NF{-}κB_n(t),$$

$$IκBβ_n\ NF{-}κBn'(t) = a5\ IκBβ_n(t)\ \ NF{-}κBn(t) - d5\ IκBβ_n\ NF{-}κBn(t) - 0.5\ k2\ IκBβ_n\ NF{-}κB_n(t),$$

$$IκBε_n\ NF{-}κB_n'(t) = a6\ IκBε_n(t)\ \ NF{-}κB_n(t) - d6\ IκBε_n\ NF{-}κB_n(t) - 0.5\ k2\ IκBε_n\ NF{-}κB_n(t),$$

Free cytoplasmic IKK protein
Accounting for adaptation to the signal, binding rates and IκB degradation due to IKK activity.

$$IKK'(t) = -k02\ IKK(t) - a1\ IKK(t)\ I\kappa B\alpha(t) + (d1 + r1)\ IKKI\kappa B\alpha(t) - a2\ IKK(t)\ I\kappa B\beta(t) + (d2 + r2)\ IKKI\kappa B\beta(t) - a3\ IKK(t)\ I\kappa B\varepsilon(t) + (d3 + r3)\ IKKI\kappa B\varepsilon(t) - a7\ IKK(t)\ I\kappa B\alpha\ NF{-}\kappa B(t) + (d1 + r4)\ IKKI\kappa B\alpha\ NF{-}\kappa B(t) - a8\ IKK(t)\ I\kappa B\beta\ NF{-}\kappa B(t) + (d2 + r5)\ IKKI\kappa B\beta\ NF{-}\kappa B(t) - a9\ IKK(t)\ I\kappa B\varepsilon\ NF{-}\kappa B(t) + (d3 + r6)\ IKKI\kappa B\varepsilon\ NF{-}\kappa B(t),$$

Cytoplasmic IKK-IκB complexes
Accounting for binding rates and IκB degradation due to IKK activity.

$$IKKI\kappa B\alpha'(t) = a1\ IKK(t)\ I\kappa B\alpha(t) - (d1 + r1)\ IKKI\kappa B\alpha(t) - a4\ IKKI\kappa B\alpha(t)\ \ NF{-}\kappa B(t) + d4\ IKKI\kappa B\alpha\ NF{-}\kappa B(t),$$

$$IKKI\kappa B\beta'(t) = a2\ IKK(t)\ I\kappa B\beta(t) - (d2 + r2)\ IKKI\kappa B\beta(t) - a5\ IKKI\kappa B\beta(t)\ \ NF{-}\kappa B(t) + d5\ IKKI\kappa B\beta\ NF{-}\kappa B(t),$$

$$IKKI\kappa B\varepsilon'(t) = a3\ IKK(t)\ I\kappa B\varepsilon(t) - (d3 + r3)\ IKKI\kappa B\varepsilon(t) - a6\ IKKI\kappa B\varepsilon(t)\ \ NF{-}\kappa B(t) + d6\ IKKI\kappa B\varepsilon\ NF{-}\kappa B(t),$$

Cytoplasmic IKK-IκB-NF-κB complexes
Accounting for binding rates between IKK-IκB complexes and NF-κB, as well as IκB-NF-κB complexes and IKK, and IκB degradation due to IKK activity.

$$IKKI\kappa B\alpha\ NF{-}\kappa B'(t) = \ a7\ IKK(t)\ I\kappa B\alpha\ NF{-}\kappa B(t) + a4\ IKKI\kappa B\alpha(t)\ \ NF{-}\kappa B(t) - (d1 + d4 + r4)\ IKKI\kappa B\alpha\ NF{-}\kappa B(t),$$

$$IKKI\kappa B\beta\ NF{-}\kappa B'(t) = \ a8\ IKK(t)\ I\kappa B\beta\ NF{-}\kappa B(t) + a5\ IKKI\kappa B\beta(t)\ \ NF{-}\kappa B(t) - (d2 + d5 + r5)\ IKKI\kappa B\beta\ NF{-}\kappa B(t),$$

$$IKKI\kappa B\varepsilon\ NF{-}\kappa B'(t) = \ a9\ IKK(t)\ I\kappa B\varepsilon\ NF{-}\kappa B(t) + a6\ IKKI\kappa B\varepsilon(t)\ \ NF{-}\kappa B(t) - (d3 + d6 + r6)\ IKKI\kappa B\varepsilon\ NF{-}\kappa B(t),$$

I. PARAMETER VALUES IN THE LITERATURE

1. IκB mRNA and protein half-lifes

The IκB mRNA half-life is estimated to be 30min. - 2 hrs. (11), which constrains the rate constant for IκB mRNA transcript degradation to 0.0004 s^{-1} to 0.0001 s^{-1}.

IκB protein half-life (signal-independent) complexed to NF-κB: 550 min; half-life of free IκB: 110 min.(3)
The rate of constitutive IκB degradation when bound to NF-κB is ln2/(550*60 s) = 0.00002 s^{-1}
and when not bound to NF-κB is ln2/(110*60 s) = 0.0001 s^{-1}.

2. Interactions between IKK, IκB and NF-κB

IKK-IκB interaction (in the absence of NF-κB):
The following data are from (4).

Table 1: Kinetics for the interaction between IKK2 and the IκB Isoforms

IκB isoform	k_a (M^{-1} s^{-1})	k_d (s^{-1})	$K_D{}^a$ (M) = k_d/k_a
IκBα	22.5 (±2.5) _ 10^3	1.25 (±0.15) _ 10^{-3}	56 _ 10^{-9}
IκBβ1	10.5 (±1.5) _ 10^3	1.25 (±0.15) _ 10^{-3}	119 _ 10^{-9}
IκBβ2	6.0 (±1.0) _ 10^3	1.75 (±0.15) _ 10^{-3}	292 _ 10^{-9}
IκBε	9.0 (±2.0) _ 10^3	1.75 (±0.15) _ 10^{-3}	194 _ 10^{-9}

Table 2: Kinetic parameters K_M and k_{cat} for the phosphorylation of the IκB isoforms by IKK

IκB isoform	K_M (M)	$k_{cat}{}^a$ (s^{-1})	$k_{cat}/K_M{}^b$ (s^{-1} M^{-1})
IκBα	1.7 (±0.6) _ 10^{-6}	3.7 _ 10^{-2}	22 _ 10^3
IκBβ1	3.2 (±1.1) _ 10^{-6}	3.2 _ 10^{-2}	10 _ 10^3
IκBβ2	2.8 (±1.0) _ 10^{-6}	1.5 _ 10^{-2}	5.4 _ 10^3
IκBε	2.6 (±0.4) _ 10^{-6}	2.2 _ 10^{-2}	8.5 _ 10^3

It is reported in (5) that $k_{cat}{}^a \approx 10^{-2}$ s^{-1} and K_M = 0.6-1 μM in general agreement with the values above.

These values allow us to deduce rate constants for associations dissociation and catalysis:

IκB isoform	k_a (μM^{-1} s^{-1})	k_d (s^{-1})	k_{cat} (s^{-1})
IκBα	22.5 _ 10^{-3}	1.25 _ 10^{-3}	3.7 _ 10^{-2}
IκBβ	6.0 _ 10^{-3}	1.75 _ 10^{-3}	1.5 _ 10^{-2}
IκBε	9.0 _ 10^{-3}	1.75 _ 10^{-3}	2.2 _ 10^{-2}

IKK-IκB interaction (in the presence of NF-κB):

The existence of the tripartite IKK-IκB-NF-κB complex has been demonstrated in (1).
Zandi et al. report that "Kinetic analysis indicated that in the presence of NF-κB, the K_m for IκB phosphorylation by IKK decreased from 2.2 μM to 1.4 μM and the relative maximum initial velocity V_{max} (or $k_{cat}{}^{a}$) was increased by a factor of 5." (2)

Thus we conclude that in the presence of NF-κB k_{cat} is increased by a factor of 5, and k_a is increased 7-8-fold:

IκB isoform	k_a (μM^{-1} s^{-1})	k_d (s^{-1})	k_{cat} (s^{-1})
IκBα	$1.85 \_ 10^{-1}$	$1.25 \_ 10^{-3}$	$1.85 \_ 10^{-1}$
IκBβ	$4.8 \_ 10^{-2}$	$1.75 \_ 10^{-3}$	$7.5 \_ 10^{-2}$
IκBε	$7.0 \_ 10^{-2}$	$1.75 \_ 10^{-3}$	$1.1 \_ 10^{-1}$

IκB-NF-κB interactions:

Affinity is estimated as being on the order of 1 nM (6), with the dissociation rate constant assumed to be around 0.001 s^{-1} in (7), and association and dissociation rate constants estimated at 18.4 $\mu M^{-1}min^{-1}$ and 0.055min^{-1} in (6). There is no data on differential affinity constants for IκB isoforms.

Though these values are somewhat conflicting, they constrain our parameter fitting to k_a = 0.3 μM^{-1} s^{-1} - 1 μM^{-1} s^{-1} and k_d = 0.0003 s^{-1} - 0.001 s^{-1}.

3. Cytoplasmic-Nuclear Transport

The transport characteristics of IκB and NF-κB and the concentration of NF-κB are examined in (7). While IκBα-NF-κB complexes are largely cytoplasmic, free NF-κB is largely nuclear. IκBα overexpression studies suggest that the ratio of the transport parameters is $k_{imp}/k_{exp} \sim 2$. We assume that to be the same for IκBβ and –ε.
The time constant of the nuclear import of IκBα is estimated to be within the 0.01-0.07 min^{-1} range. These observations constrain IκB import to 1.7-11.7 10^{-4} s^{-1} and IκB export to 0.8 - 5.8 10^{-4} s^{-1}.

It is also noted in (7) and (8) that IκB-NF-κB complex dissociates such that IκB and NF-κB to enter the nucleus independently, which means that nuclear import of the IκB-NF-κB complex is zero.

When nuclear export is blocked with the small molecule inhibitor leptomycin B, IκBβ and IκBε show significantly less nuclear accumulation than IκBα (10). To reflect that observation, we multiplied the relevant transport terms by a factors of 0.4 or 0.5 in the equations.

However, upon TNF stimulation newly synthesized IκBβ accumulates in the nucleus, binding NF-κB-DNA complexes (9). To account for this phenomenon, we have included a term that controls the fraction of IκBβ molecules that are subject to export with respect to time: `fr'[t]=-.5/(1+t)^2, fr[0]=.5`

II. MODEL FITTING PROCEDURES FOR PARAMETER ESTIMATION

Introduction

Most parameter values in the model have been taken directly from the literature, as described above. Other parameter values are constrained by published results. The parameters that were varied during model fitting to the experimental data in Fig. 2 were the rates of transcription and translation of IκB isoforms and the rate of IκB–NF-κB nuclear export and NF-κB nuclear import. Note that, since only one IκB isoform is present in each knockout cell line, the rates of synthesis of each given isoform can be adjusted independently. The rates of translation were assumed to be equal for all isoforms involved. In the parameter estimation it was determined that an increase in the rates of IκB isoform transcription could be almost exactly compensated by a proportional decrease in the rate of translation. The translation rate was chosen to correspond to a 3-4 min. time constant.

In adjusting the parameters, it is common to use techniques leading to minimization of the sum of squares of the differences between the predicted and actual responses. Among these methods are the gradient descent method, the Levenberg-Marquardt method, the direct search method of Hooke and Jeeves, etc. (see (12) for extended reference list and discussion). However, given a sufficiently complex biochemical network the performance of these methods can be quite poor (13). In addition, these fitting techniques applied to oscillatory behavior skew towards optimizing frequency matches rather than amplitude and overall qualitative shape of the curve, since a small shift in frequency (and the time of the onset of the oscillations) can lead to a substantial increase in the sum of residuals. On the other hand the fitting process is already significantly constrained by the values for previously published parameters.

Reduced model fitting to knock-out cell line data

We first utilized the steepest gradient descent (GD), genetics algorithm (GA) and random search parameter estimation in the Gepasi version 3.1 software package. Random search parameter estimation yielded the best results among several fitting methods as evidenced by the standard deviation of the estimated parameter values. The most challenging model fitting task represents the oscillatory NF-κB activation profile in IκBβ-/-IκBε-/- cells. As shown in Fig.S1, there is satisfactory fit at early time points, but the resulting model fails to describe faithfully the overall shape and frequency of oscillations. In particular, there is a considerable overestimation of the degree of the oscillation damping.

Next, we used the parameter estimates derived from the random method and varied them within the standard deviation limits to improve the qualitative fits regarding frequency and amplitude of oscillations. Such qualitative fitting led to a 6% decrease in the estimate of the transcription rate and about a two-fold decrease in the IκB-NF-κB nuclear export rate (the model was rather insensitive to variations of the latter). The estimate for the NF-κB nuclear import rate was not readjusted.

Both the IκBα transcription rate and the rate of IκB-NF-kB nuclear export affect the frequency and the amplitude (the degree of damping) of the oscillations. We have varied these parameters, as described above. Similarly, we studied the behavior of the models, in which only IκBβ and IκBε are expressed (these “knockout” models are generated by equating the rates of transcription for two IκB isoforms out of three to zero). These studies resulted in the simulation curves presented in Fig. 2 of the paper.

Wild type cell model fitting

To generate the model of the wild type fibroblast response, we first assumed that we can simply equate the transcription rates for all IκB isoforms to the values determined in double knockout fitting studies. However, as shown in Fig. 2D, these results failed to agree with the experimental data. The model output was fitted to the wild type cell experimental data by adjusting the transcription rates for IκBβ and IκBε only. These rates were adjusted down 7-fold to result in good qualitative approximation of the wild type behavior. We concluded that it is likely that there is a cross-regulation between IκB isoforms leading to compensation of the absence of IκB isoforms in the knockout lines through up-regulation of the existing IκB isoform. Such parameter adjustment emphasizes that variation of the rates of synthesis of β and ε isoforms can lead to significant changes in the signaling characteristics.

Conclusion

The goal of this study is not an exact estimation of biochemical parameters. Parameter sensitivity studies (A.L. unpublished results) can explore how error in the estimates may affect the system's response. Importantly, the conclusions of our study regarding the respective functions of IκB isoforms, the bimodal signal processing characteristics, and the newly revealed mechanism for specificity in gene expression are not dependent on exact parameter estimates. This also suggests that these conclusions are valid in a variety of cell types, physiological or experimental conditions where parameter values may differ.

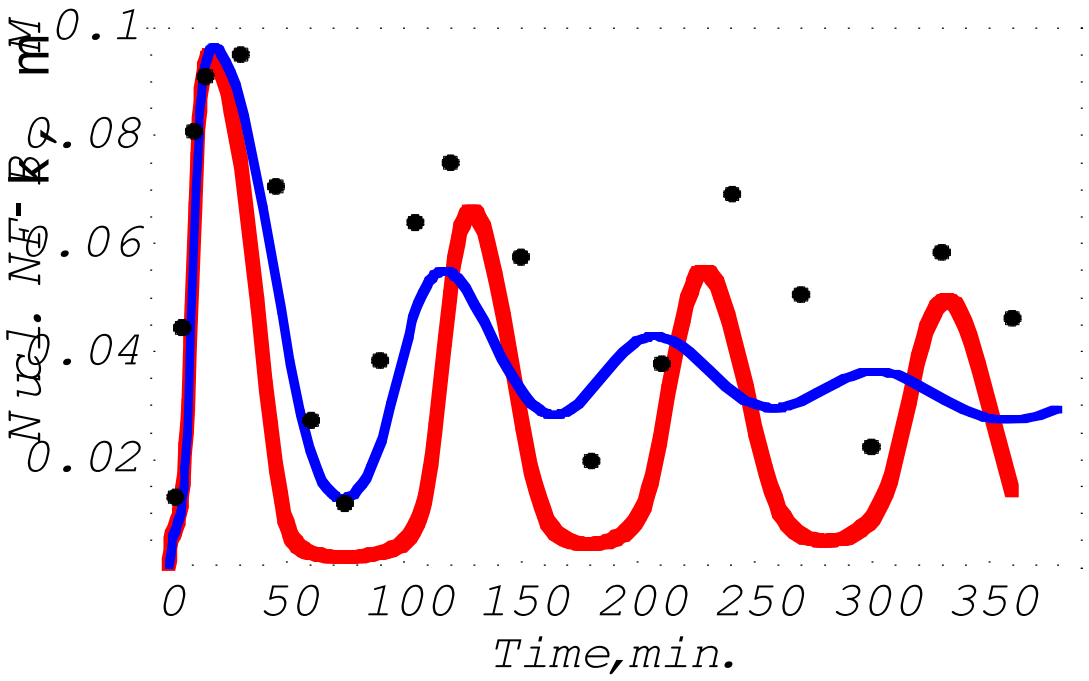

Fig. S1 Comparison of the fitting methods applied to the oscillatory NF-κB activation profile in IκBβ-/-IκBε-/- cells. The experimental data are shown as black filled circles, the "semi-quantitative" fit is shown in red and the result of random search fitting in blue. The fitting was performed using the fitting engines supplied with the Gepasi package, version 3.1 (11).

REFERENCES

1. Heilker, R., F. Freuler, R. Pulfer, F. Di Padova, and J. Eder. 1999. All three IκB isoforms and most Rel family members are stably associated with the IκB kinase 1/2 complex. *Eur.J.Biochem.* 259:253-261.

2. Zandi, E., Y. Chen, and M. Karin. 1998. Direct phosphorylation of IκB by IKKα and IKKβ: discrimination between free and NF-κB-bound substrate. *Science* 281:1360-1363.

3. Pando, M.P. and I.M. Verma. 2000 Signal-dependent and -independent degradation of free and NF-κB-boundound IκBα. *J.Biol.Chem. 275:21278-86.*

4. Heilker, R., F. Freuler, M. Vanek, R. Pulfer, T. Kobel, J. Peter, H.G. Zerwes, H. Hofstetter, and J. Eder. 1999. The kinetics of association and phosphorylation of IκB isoforms by IκB kinase 2 correlate with their cellular regulation in human endothelial cells. *Biochemistry* 38:6231-6238.

5. Huynh, Q.K., H. Boddupalli, S.A. Rouw, C.M. Koboldt, T. Hall, C. Sommers, S.D. Hauser, J.L. Pierce, R.G. Combs, B.A. Reitz, J.A. Diaz-Collier, R.A. Weinberg, B.L. Hood, B.F. Kilpatrick, and C.S. Tripp. 2000. Characterization of the recombinant IKK1/IKK2 heterodimer. Mechanisms regulating kinase activity. *J.Biol.Chem..* 275:25883-25891.

6. Malek, S., T. Huxford, and G. Ghosh. 1998. IκBα functions through direct contacts with the nuclear localization signals and the DNA binding sequences of NF-κB. *J.Biol.Chem.* 273:25427-25435.

7. Carlotti, F., S.K. Dower, and E.E. Qwarnstrom. 2000. Dynamic shuttling of nuclear factor kappa B between the nucleus and cytoplasm as a consequence of inhibitor dissociation. *J.Biol.Chem.* 275:41028-41034.

8. Birbach, A., Gold, P., Binder, B.R., Hofer, E., de Martin, R., and Schmid**,** J.A. 2002. Signaling Molecules of the NF-κB pathway shuttle constitutively between cytoplasm and nucleus . *J.Biol.Chem.* 277:10842-10851.

9. Tam WF, Sen R. 2001. IκB family members function by different mechanisms. *J. Biol. Chem*. 276:7701-4.

10. Suyang, H., Phillips, R., Douglas, I., Ghosh, S. 1996 Role of unphosphorylated, newly synthesized IκBβ in persistent activation of NF-κB. Molec. Cell. Biol. 16:5444-5449.

11. Blattner C, Kannouche P, Litfin M, Bender K, Rahmsdorf HJ, Angulo JF, Herrlich P. 2000. UV-Induced stabilization of c-fos and other short-lived mRNAs. *Mol Cell Biol.* 20:3616-25.

12. Mendes, P. (1993) GEPASI: a software package for modelling the dynamics, steady states and control of biochemical and other systems. Comput. Appl. Biosci. 9, 563-571; Mendes, P. (1997) Biochemistry by numbers: simulation of biochemical pathways with Gepasi 3. Trends Biochem. Sci. 22, 361-363; Mendes, P. & Kell, D. B. (1998) Non-linear optimization of biochemical pathways: applications to metabolic engineering and parameter estimation. Bioinformatics 14, 869-883

13. P. Mendes. Modeling large biological systems from functional genomic data: parameter estimation. in Foundations of Systems Biology, ed. H. Kitano, MIT Press, pp. 163-181 (2001)

III. SUMMARY OF PARAMETER VALUES

We have indicated by **black color** the values that were previously determined experimentally, and by **blue color** the values that were constrained by published results. Values in **red color** were derived de novo during model fitting to our experimental data from cells harboring genetically reduced and wild-type IκB-NF-κB signaling modules.

Two component interactions:	**Symbol:**	**Values:**	**Units:**
IκBα-NF-κB association	a4	$0.5 \_ 10^{0}$	$\mu M^{-1} s^{-1}$
IκBα-NF-κB dissociation	d4	$0.5 \_ 10^{-3}$	s^{-1}
IκBβ-NF-κB association	a5	$0.5 \_ 10^{0}$	$\mu M^{-1} s^{-1}$
IκBβ-NF-κB dissociation	d5	$0.5 \_ 10^{-3}$	s^{-1}
IκBε-NF-κB association	a6	$0.5 \_ 10^{0}$	$\mu M^{-1} s^{-1}$
IκBε-NF-κB dissociation	d6	$0.5 \_ 10^{-3}$	s^{-1}
IKK-IκBα association	a1	$22.5 \_ 10^{-3}$	$\mu M^{-1} s^{-1}$
IKK-IκBα dissociation	d1	$1.25 \_ 10^{-3}$	s^{-1}
IKK-IκBα catalysis	r1	$3.7 \_ 10^{-2}$	s^{-1}
IKK-IκBβ association	a2	$6.0 \_ 10^{-3}$	$\mu M^{-1} s^{-1}$
IKK-IκBβ dissociation	d2	$1.75 \_ 10^{-3}$	s^{-1}
IKK-IκBβ catalysis	r2	$1.5 \_ 10^{-2}$	s^{-1}
IKK-IκBε association	a3	$9.0 \_ 10^{-3}$	$\mu M^{-1} s^{-1}$
IKK-IκBε dissociation	d3	$1.75 \_ 10^{-3}$	s^{-1}
IKK-IκBε catalysis	r3	$2.2 \_ 10^{-2}$	s^{-1}

Three component interactions:	**Symbol:**	**Values:**	**Units:**
IKK-IκBαNF-κB association	a7	$1.85 \_ 10^{-1}$	$\mu M^{-1} s^{-1}$
IKK-IκBαNF-κB dissociation	d1	$1.25 \_ 10^{-3}$	s^{-1}
IKKIκBα-NF-κB association	a4	$0.5 \_ 10^{0}$	$\mu M^{-1} s^{-1}$
IKKIκBα-NF-κB dissociation	d4	$0.5 \_ 10^{-3}$	s^{-1}
IKKIκBαNF-κB catalysis	r4	$1.85 \_ 10^{-1}$	s^{-1}
IKK-IκBβNF-κB association	a8	$4.8 \_ 10^{-2}$	$\mu M^{-1} s^{-1}$
IKK-IκBβNF-κB dissociation	d2	$1.75 \_ 10^{-3}$	s^{-1}
IKKIκBβ-NF-κB association	a5	$0.5 \_ 10^{0}$	$\mu M^{-1} s^{-1}$
IKKIκBβ-NF-κB dissociation	d5	$0.5 \_ 10^{-3}$	s^{-1}
IKKIκBβNF-κB catalysis	r5	$7.5 \_ 10^{-2}$	s^{-1}
IKK-IκBεNF-κB association	a9	$7.0 \_ 10^{-2}$	$\mu M^{-1} s^{-1}$
IKK-IκBεNF-κB dissociation	d3	$1.75 \_ 10^{-3}$	s^{-1}
IKKIκBε-NF-κB association	a6	$0.5 \_ 10^{0}$	$\mu M^{-1} s^{-1}$
IKKIκBε-NF-κB dissociation	d6	$0.5 \_ 10^{-3}$	s^{-1}
IKKIκBεNF-κB catalysis	r6	$1.1 \_ 10^{-1}$	s^{-1}

Synthesis and degradation:	Symbol:	Values:	Units:
IκBα inducible mRNA synthesis	tr2	1.7 _ 10^{-1}	μM^{-1} s^{-1}
IκBα constitutive mRNA synthesis	tr2a	1.5 _ 10^{-6}	μM s^{-1}
IκBβ constitutive mRNA synthesis	tr2b	2.3 _ 10^{-7}	μM s^{-1}
IκBε constitutive mRNA synthesis	tr2e	1.7 _ 10^{-7}	μM s^{-1}
IκB mRNA degradation	tr3:	2.8 _ 10^{-4}	s^{-1}
constitutive IκB translation rate	tr1	4 _ 10^{-3}	s^{-1}
constitutive IκB degradation (free)	deg1	1.0 _ 10^{-4}	s^{-1}
constitutive IκB degradation (complexed to NF-_B)	deg2	2.1 _ 10^{-5}	s^{-1}

Nucleo-cytoplasmic transport:	Symbol:	Values:	Units:
IκBα nuclear import	tp1	3 _ 10^{-4}	s^{-1}
IκBα nuclear export	tp2	2 _ 10^{-4}	s^{-1}
IκBβ nuclear import	0.5 tp1	1.5 _ 10^{-4}	s^{-1}
IκBβ nuclear export `fr'[t]=-.5/(1+t)^2`	0.5 tp2	1 _ 10^{-4}	s^{-1}
IκBε nuclear import	0.5 tp1	1.5 _ 10^{-4}	s^{-1}
IκBε nuclear export	0.5 tp2	1 _ 10^{-4}	s^{-1}
NF-κB nuclear import	k1	0.9 _ 10^{-1}	s^{-1}
NF-κB nuclear export	k01	0.8 _ 10^{-4}	s^{-1}
IκBα-NF-κB nuclear export	k2	1.4 _ 10^{-2}	s^{-1}
IκBβ-NF-κB nuclear export `fr'[t]=-.5/(1+t)^2`	0.4 k2	5.6 _ 10^{-3}	s^{-1}
IκBε-NF-κB nuclear export	0.4 k2	5.6 _ 10^{-3}	s^{-1}

Simulation protocol

As we are considering "active" IKK, all simulations are started with IKK concentration equal to zero. Following "equilibration" for 2000 min., IKK is raised as a step function to 0.1 μM. We assume that following the signal onset there is a slow adaptation (k02 = 8.3_10^{-5} s^{-1}; half-life of 2.3 hrs.), gradually reducing active IKK concentration.

Signal removal (corresponding to experimental wash of cells to remove TNF) is modeled as adjustment of the adaptation coefficient k02 to 2.3_10^{-3} s^{-1} (half-life of 5 min.).

BIOCHEMICAL AND MOLECULAR BIOLOGICAL METHODS

Cell lines and cell culture

Human JURKAT and U937 cell lines were grown in DMEM with 10% fetal calf serum and stimulated with 10ng/ml human TNFα (Biogen). Immortalized fibroblast cell lines were made from E14.5 embryos according to the 3T3 protocol in 10% calf serum (S.A. Aaronson and G.J. Todaro 1968, J. Cell. Phyisol. vol. 72, pp. 141-148) and maintained in the same manner. Subconfluent or confluent-and-starved (0.5% serum) cells in 10cm polylysine-coated dishes were stimulated with 10ng/ml murine TNFα (Roche).

Electrophoretic Mobility Shift Assay (EMSA)

Following a wash with ice cold phosphate buffered saline (PBS) supplemented with 1mM EDTA, cells were collected (scraped with a rubber policeman, if necessary) into a microfuge tube tube and pelleted at 2000g. Cells (about 10^6) were resuspended and allowed to swell in 100µl CE buffer (10mM Hepes-KOH pH7.9, 60mM KCl, 1mM EDTA, 0.5% NP-40, 1mM DTT, 1mM PMSF) and vortexed for lysis. Nuclei were pelleted at 4000g, and cytoplamic lysate removed for SDS-PAGE (following protein concentration normalization) and standard Western blot analysis. Antibodies from Santa Cruz Biotechnology, Inc were used for IκBα (sc-371) and IκBβ (sc-945). A mouse polyclonal antibody was prepared against full-length recombinant mouse IκBε protein according to standard procedures. For EMSA, Nuclei were resuspended in 30µl NE buffer (250mM Tris pH7.8, 60mM KCl, 1mM EDTA, 1mM DTT, 1mM PMSF) and lysed by 3 freeze-thaw cycles. Nuclear lysates are cleared by 14000g centrifugation and adjusted to 1µg/µl total protein concentation following Bradford assay. 2µg of total nuclear protein was reacted at room temperature for 15min. to 0.1pmoles of P32-labelled 30pb double-stranded oligonucleotide containing a consensus κB-site (AGCTTGCTACAA**GGGACTTTCC**GCTGTCTACTTT) in 6µl binding buffer (10mM Tri.Cl pH7.5, 50mM NaCl, 10% glycerol, 1% NP-40, 1mM EDTA, 0.1µg/µl polydIdC). Complexes were resolved on a non-denaturing 5% acrylamide (30:0.8) gel containing 5% glycerol and 1x TGE (24.8mM Tris, 190mM glycine, 1mM EDTA) and visualized by standard autoradiography and/or quantitated using a Phosphoimager (Molecular Dynamics), in which the unbound probe (>20 fold excess) was used to normalize for loading variability. Graphed data is 1000x(signal–background)/(unbound probe–background).

RNAse Protection Assay (RPA)

Total RNA was made from confluent and starved fibroblasts using Tri-Reagent (Molecular Research Center, Inc). RNase Protection Analysis was performed with 5µg RNA using Riboquant probe set mCK-5 (Pharmingen) according to manufacturers instructions.

Generation of the IkBε-/- mouse.

The targeting construct results in a deletion of Amino acids 145-343 of IκBε and hence disruption of all 6 ankyrin repeats. Standard methods were utilized in the ES cell selection, the deletion blastocyst injections and derivation of a knock-out mouse strain. The targeting construct was generated as follows:

1. Two overlapping clones spanning approximately 20 kb of 129SvJ genomic DNA and containing the entire IκBε coding sequence were subcloned from lambda FIXII (Stratagene) into pBSK(+). These subclones, referred to as 8A21H and 10A44, were extensively mapped by restriction digestion and oligonucleotide hybridization.

2. A 2.0 kb Bgl2-Xho1 fragment from 8A21H that contained the first coding exon of IκBε was blunted with Klenow polymerase and gel isolated. The fragment was then ligated to a Pme1-digested knockout vector, pLNTKP (kindly provided by F. Alt). This yielded a cloning intermediate called pEK1. The presence of IκBε coding nucleotides 1-345 just upstream of the neomycin resistance cassette, at the (Xho1)-vector junction of pEK1, was confirmed by DNA sequencing.

3. Oligonucleotide linkers containing a Xho1 recognition site were ligated to a 7.3 kb Bgl2 fragment of subclone 10A44 ; the fragment was gel purified and cut with Xho1. This fragment was then ligated to pEK1 DNA previously treated with Xho1 and alkaline phosphatase to give a final knockout construct, pEK7.

4. DNA sequencing of pEK7, beginning in the neomycin resistance cassette and extending downstream into genomic DNA, revealed an exon composed of coding nucleotides 1029-1102 of IκBε. The intron/exon sequence of the deleted portion of genomic DNA was not determined. Therefore, intervening exons are not indicated in the accompanying diagram.

5. The pEK7 construct was linearized with Pac1 and introduced into E14 ES cells by standard methods. A hybridization probe derived from an upstream Bgl2-EcoRV fragment was used to screen HindIII-digested DNA from neo-resistant ES cell colonies as indicated in the accompanying diagram.